ELSEVIER

Nuclear Instruments and Methods in Physics Research B 171 (2000) 325–331

NIM B
Beam Interactions with Materials & Atoms

www.elsevier.nl/locate/nimb

Au–Si eutectic alloy formation by Si implantation in polycrystalline Au

V. John Kennedy, G. Demortier *

Laboratoire d'Analyses par Reactions Nucleaires (LARN), Facultés Universitaires Notre-Dame de la Paix, rue de bruxelles 61, B-5000 Namur, Belgium

Received 24 February 2000; received in revised form 18 May 2000

Abstract

Different doses of high-energy Si (0.2–4.5 MeV) were implanted in polycrystalline Au foils (35 μm thick) to form a low melting point Au–Si alloy which can be used for gold soldering. A Au–Si eutectic structure has been observed in the implanted Au foils after annealing at 400°C for 1 h. The Au–Si liquid phase was diffused in the polycrystalline Au foil along the grain boundaries which were flattened by the initial rolling procedure. The presence of this eutectic alloy was also observed on the back of the Au foil. Nuclear (d,p) reactions induced by deuterons have been used to measure the concentration of the implanted Si in various depths in the Au foils. RBS was also used as a complementary technique to probe the Au concentration. SEM pictures indicate that an eutectic structure was induced in the implanted samples.

Keywords: Au–Si; NRA; RBS; Si implantation; SEM

1. Introduction

Gold–silicon structures are considered to be important systems and are extensively studied owing to their technological properties. It has been shown that Si atoms are dislodged from Si/Au interface at a low temperature and migrate through Au. This effect has been widely studied for Au films deposited on Si crystals. The diffusion process takes place at low temperature involving the formation of Au silicide. At a temperature above the Au–Si eutectic temperature (363°C), the interaction between the Au film and the Si substrate leads to the formation of an alloy rather than Au silicide. It has been established that silicon alloyed with gold may form an eutectic alloy which can be used as a low melting point solder for silicon devices [1,2]. High diffusion rates of silicon in gold film coatings on silicon crystals have been widely studied by various groups [3,4].

In the last few years, we have experimented with a process of gold soldering involving two steps: (i) the formation of a microscopic Au–Si eutectic alloy during silicon diffusion through the

* Corresponding author. Tel.: +32-81-725475; fax: +32-81-725474.

E-mail address: guy.demortier@fundp.ac.be (G. Demortier).

0168-583X/00/$ - see front matter
PII: S0168-583X(00)00290-1

grain boundaries of polycrystalline Au foils from a thin film of Si deposited on polycrystalline Au foil and (ii) the redistribution of a part of this eutectic alloy for joining with a second piece of Au. Both steps were performed at a temperature slightly higher than the eutectic temperature [5,6]. The aim of the present study is to present an alternative procedure for the formation of the Au–Si eutectic alloy by diffusion of Si-implanted polycrystalline Au foils followed by a thermal diffusion. Nuclear reactions induced by a deuteron beam have been used to characterize the Au–Si alloy formed by diffusion of Si into Au foils. Metallographic images were obtained by scanning electron microscopy (SEM).

2. Experimental procedure

2.1. Implantation

Pure (99.99%) polycrystalline Au foils were rolled at room temperature down to thickness of 40 μm. The foils were implanted with Si^{2+} ions using a 2 MV Tandetron Accelerator of LARN. The implanted area was around 0.04 cm^2. The Au foils were kept tight in a frame made of brass and mounted on a target ladder which is connected to the current integrator. Different doses (1×10^{17}, 3×10^{17}, 4×10^{17}, 6×10^{17} at./cm^2) were implanted in different Au foils (35 μm thick) to optimize the doses required to achieve the eutectic alloy composition (19 at.% of Si in Au). In order to study the Si depth profile in Au, samples were also prepared with three different energies of Si ions (220 keV, 2 MeV, 4.5 MeV). Using the TRIM code [7], the expected Si implantation ranges in Au for the above energies were calculated and found to be 88, 730 and 1300 nm; the doses were calculated to achieve the eutectic composition.

2.2. Characterization

Proton spectroscopy induced by the exoenergetic $^{28}Si(d,p)^{29}Si$ nuclear reaction has been used to analyze the silicon depth profile in the Au foils. The incident deuterons may approach the silicon nuclei at a sufficiently close distance to induce a nuclear reaction and to give rise to an emission of energetic protons. Measuring the energy of those protons leads to a quantitative method of analysis of Si at various depths under the surface of the irradiated material. The advantages for using this technique have been explained in earlier publications [8,9]. A beam of 2.98 MeV deuterons was focused (1 mm^2) on the Si-implanted Au foils. An SSB detector (12 keV FWHM, active area 25 mm^2) was placed at a backscattering angle of 165° at a distance of 60 mm from the beam spot. The detection angle (165°) has been chosen to use the published cross-section values [10,11]. An absorber foil of Mylar (78 μm) was placed in front of the detector to stop the backscattered deuterons. Another SSB detector (12 keV FWHM) was placed at a backscattered angle of 135° to collect the backscattered deuterons. Measurements were carried out in the implanted samples. Subsequently the samples were annealed at 400°C for 15 min and 1 h, respectively, and the measurements were repeated under the same experimental conditions. The temperature of annealing was slightly higher than the eutectic temperature (363°C) so that any Au–Si mixture at 400°C would contain a liquid phase.

3. Results and discussion

3.1. NRA measurement

The cross-sections of $^{28}Si(d,p_0)^{29}Si$ and $^{28}Si(d,p_1)^{29}Si$ reactions at 165° given in Fig. 1 are reproduced from [11]. It can be seen that the cross-sections for the p_0 group in the energy region of 2.8 to 3 MeV varies from 1.4 to 3.0 mbarn/sr and for the p_1 group from 0.6 to 1.2 mbarn/sr.

Fig. 2 shows typical spectra of p_0 and p_1 groups induced by 2.98 MeV deuterons on the samples implanted at various energies (220 keV, 2 and 4.5 MeV). The proton energies reflect the depth at which Si has been implanted. In the case of a 4.5 MeV Si-implanted sample, p_0 and p_1 peaks are broader and the detected proton energies after crossing the absorbers are 7.52 and 6.22 MeV which correspond to an incident deuteron energy of 2.81 MeV at 1.3 μm in the depth. The p_0 and p_1

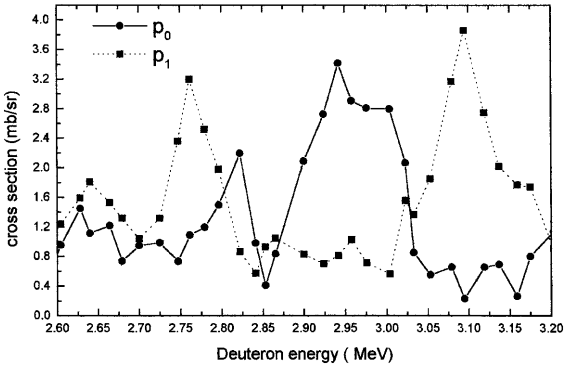

Fig. 1. Cross-sections of ^{28}Si(d,p$_0$) ^{29}Si and ^{28}Si(d,p$_1$) ^{29}Si nuclear reactions at 165° reproduced from [11].

peaks for the 2 MeV implanted sample are observed at 7.61 and 6.31 MeV corresponding to a deuteron energy of 2.92 MeV. Since for 220 keV Si, implantation in Au is almost at the surface, one sees the p_0 and p_1 narrow peaks at 7.67 and 6.37 MeV corresponding to the nominal incident deuteron energy (2.98 MeV). The implanted doses in the above three samples are close to 18–19 at.% of Si in each different depth. Due to the cross-section variations, different yields are observed in the above spectra.

The p_0 and p_1 groups induced by 2.98 MeV deuterons on the 4.5 MeV Si ion implanted (3×10^{17} at./cm^2) Au foil before and after annealing are shown in Fig. 3. The range of the Si ions is around 1.3 μm and the width is around 300 nm. After annealing at 400°C for 15 min, Si partially diffuses towards the surface and the respective peaks appear at 7.67 and 6.37 MeV which correspond to the proton groups induced by 2.98 MeV incident deuterons. The width of the p_0 and p_1 peaks are narrower after annealing for 15 min. After 1 h of annealing the Si appears completely at the Au surface and the peaks are still narrower. The measured intensity of the peaks in the sample before heating is less than that for the annealed sample due to a lower value of the cross-section. The cross-sections for the p_0 and p_1 group produced by 2.81 MeV are indeed 1.6 and 1.2 mbarn/sr, respectively (in the as-implanted sample), but at 2.98 MeV (for the annealed sample), the corresponding values are 2.6 and 0.57 mbarn/sr.

The concentration of Si atoms has been calculated based on the following relation [12]:

$$N_{\mathrm{Si}} = \frac{\cos\theta I_{\mathrm{H}}}{\Omega(\mathrm{d}\sigma/\mathrm{d}\Omega)N_{\mathrm{I}}},$$

where θ is the angle between the incident beam and the normal of the sample, I_{H} the integral or the area under the peak due to nuclear reaction, Ω the solid angle of the NRA detector, $(\mathrm{d}\sigma/\mathrm{d}\Omega)$ the cross-section of the ^{28}Si(d,p)^{29}Si nuclear reaction

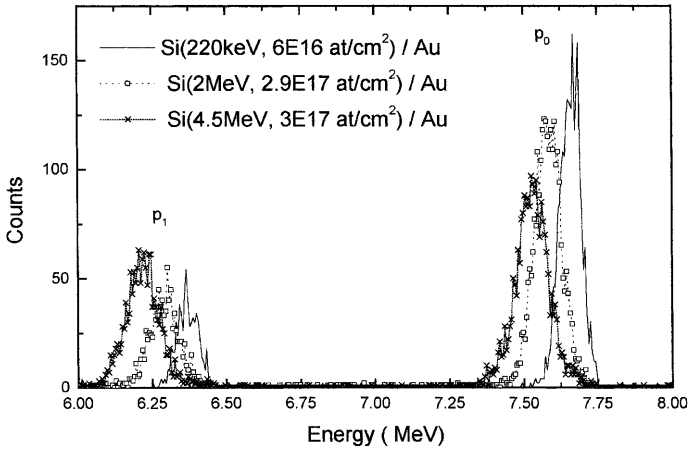

Fig. 2. Typical spectra of p_0 and p_1 groups induced by 2.98 MeV deuterons on Si-implanted polycrystalline Au foils at various Si energies.

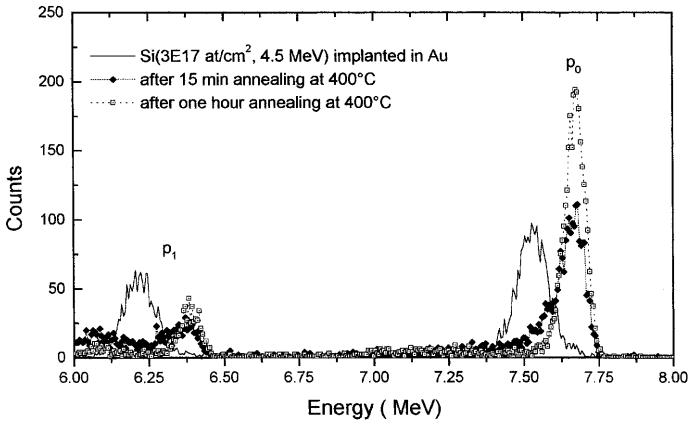

Fig. 3. Typical proton spectra (p_0 and p_1 groups) induced by 2.98 MeV deuterons on the 4.5 MeV Si-implanted (3×10^{17} at./cm^2) Au foil before and after annealing at 400°C.

and N_I is the number of incident deuterons. Using the above relation, the number of Si atoms and in the implanted sample is $2.9 \pm 0.2 \times 10^{17}$ at./cm^2 and remains the same after 1 h annealing. The calculated dose in the above sample, based on the implantation conditions, is 3×10^{17} at./cm^2. This dose corresponds to 17–19 at.% of Si in Au. The measured Si concentration for the other doses of 4.5 MeV Si-implanted samples (1×10^{17}, 4×10^{17}, 6×10^{17} at./cm^2) are also close to the calculated one.

The formation of an eutectic structure (ramifications) is observed by means of optical and electron microscopies. Fig. 4 shows an SEM micrograph of an annealed Si-implanted (4.5 MeV,

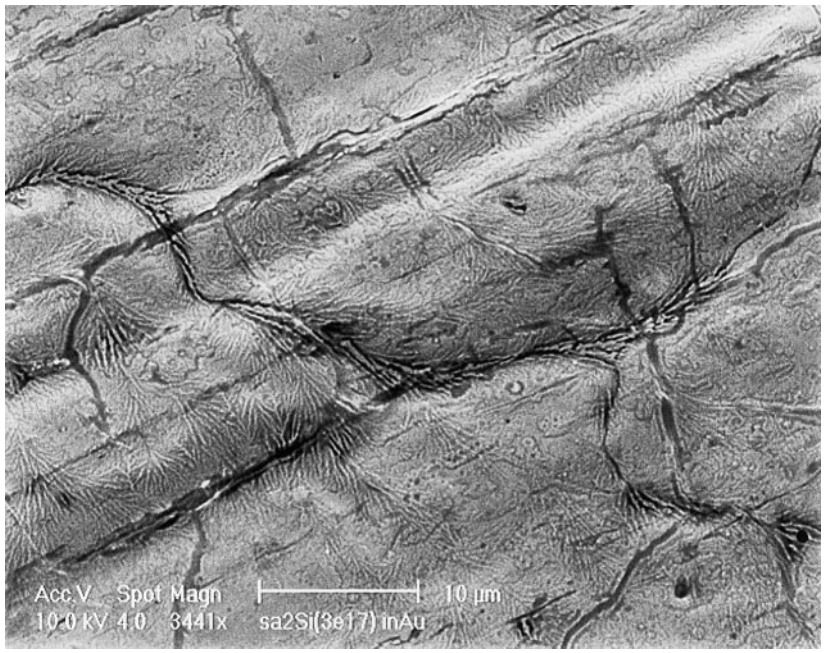

Fig. 4. SEM micrograph of the Si-implanted (4.5 MeV, 3×10^{17} at./cm^2) Au foil showing the characteristic ramifications of the eutectic alloy formed along the grain boundaries.

3×10^{17} at./cm^2) Au foil. The Au–Si liquid phase was diffused in the polycrystalline Au foil along the grain boundaries which where flattened by the initial rolling procedure. The eutectic structure is also observed in the rear part of the foil. One can indeed understand that several of the flattened grains may occupy the whole thickness of the foil and that the diffusion of the liquid phase took place through the whole thickness of the foil. The speed of diffusion is so high (a few minutes are sufficient for 35 μm thick foils) that any process of solid-state diffusion may be discarded; only migration of a liquid phase is possible. The present SEM picture is almost the same as the one observed in the Si film deposited on the Au foil, as reported earlier [5,8,9].

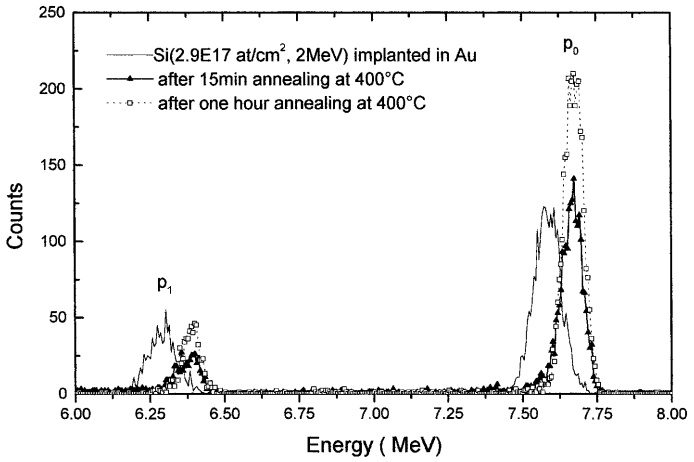

Fig. 5. Typical proton spectra (p_0 and p_1 groups) induced by 2.98 MeV deuterons on the 2 MeV Si-implanted (2.9×10^{17} at./cm^2) Au foil before and after annealing at 400°C.

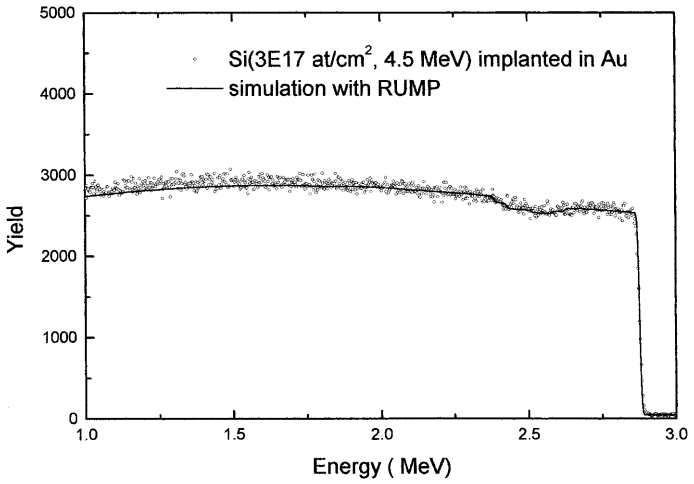

Fig. 6. Typical RBS spectra obtained in the Si-implanted (4.5 MeV, 3×10^{17} at./cm^2) Au foils using a 2.98 MeV deuteron beam and the RUMP simulations.

The p_0 and p_1 groups induced by 2.98 MeV deuteron on the Si-implanted (2 MeV, 2.9×10^{17} at./cm^2) sample is depicted in Fig. 5. The implanted range of Si is around 0.7 μm. Once more Si diffuses towards the surface in the Au foil after a few minutes of annealing at 400°C. The behavior of the diffusion is almost the same as the one observed in the 4.5 MeV Si-implanted sample. Using the relation mentioned above, the number of Si atoms after 1 h of annealing is found to be 2.8×10^{17} at./cm^2.

3.2. RBS measurement

The RBS spectrum obtained on the Si-implanted (4.5 MeV, 3×10^{17} at./cm^2) Au foil using a 2.98 MeV deutron beam is given in Fig. 6. The simulation of the RBS spectrum was obtained with the RUMP code [13]. The disappearance of Au signal in the implanted zone is clearly visible. A plot of Au concentrations versus depth is given in Fig. 7. It can be seen that the implanted region is centered around 8×10^{18} at./cm^2, which corresponds to1300 nm, a depth which is in agreement with the TRIM calculation. The difference in concentration of Au from that in the bulk corresponds to about 13–15% which is comparable with the expected eutectic composition. A concentration of around 3–5% of Si at the surface is also observed.

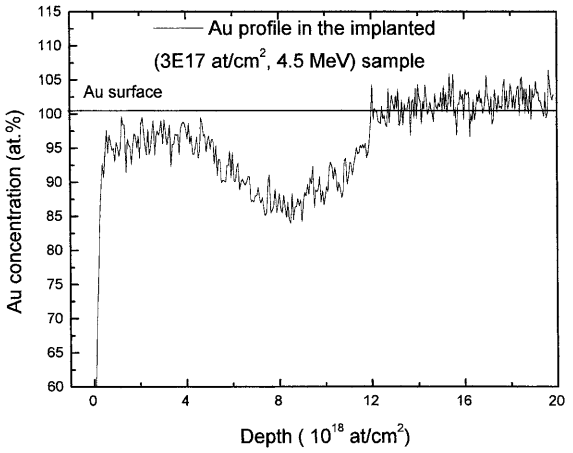

Fig. 7. Detailed plot around the implanted region of Fig. 6 to show the variation of Au concentrations versus depth.

The RBS spectrum obtained on the annealed sample (4.5 MeV, 3×10^{17} Si at./cm^2) and its comparison with the spectrum on pure Au foil are shown in Fig. 8. The corresponding RUMP simulations are also shown. The high energy edges clearly indicate that Si is at the surface but

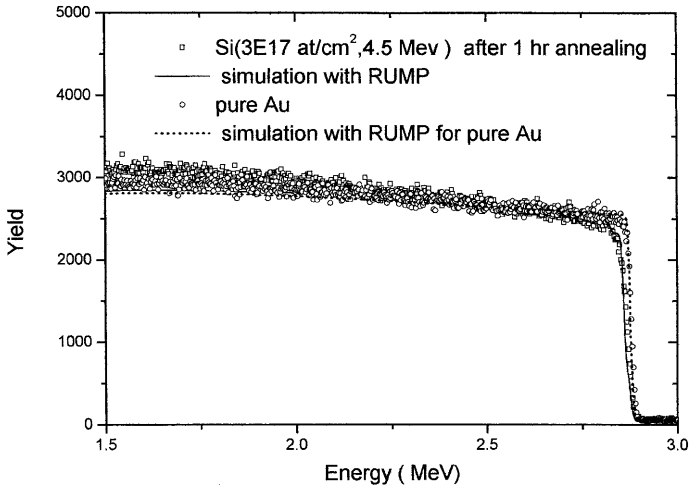

Fig. 8. Typical RBS spectra obtained for the one hour annealed sample of Si (4.5 MeV, 3×10^{17} at./cm^2) implanted Au foil and a pure Au foil. RUMP simulations for the respective spectra are also shown.

the distribution of Si is more clear using (d,p) spectra.

4. Summary and conclusions

The required dose for the formation of a Au–Si eutectic alloy by Si implantation in polycrystalline Au foils has been achieved. Using NRA induced by deuterons, the samples were characterized showing that the eutectic composition was reached in the (4.5 MeV, 3×10^{17} at./cm^2) Si-implanted Au foil. SEM micrographs give evidence for this eutectic formation. RBS has been used as a complementary technique but is less sensitive to the depth distribution than the NRA method. These implanted samples would be useful for a new procedure of soldering of gold at low temperature (400°C).

Acknowledgements

We would like to thank Dr. Guy Terwagne for his useful discussions and Mr. Yvon Morciaux for his technical assistance. We also thank Mr. Y. Houbion and Prof. P. Overlau for their contribution to obtain electron and optical microscopies.

References

[1] F.G. Yost, J. Electron. Mater. 3 (1974) 354.
[2] H. Kato, J. Electrochem. Soc. 134 (1987) 1750.
[3] A. Hiraki, Jpn. J. Appl. Phys. 22 (1983) 549.
[4] A. Cros, P. Muret, Mater. Sci. Reports 8 (1992) 271.
[5] S. Mathot, G. Demortier, in: D.J. Stephenson (Ed.), Proceedings of the Diffusion Bonding 2, Elsevier, Amsterdam, 1991, p. 302.
[6] S. Mathot, G. Demortier, Nucl. Instr. and Meth. B 49 (1990) 505.
[7] J.F. Ziegler, J.P. Biersack, U. Littmark, The Stopping and Ranges of Ions in Matter, Vol. 1, Pergamon, New York, 1985.
[8] G. Demortier, S. Mathot, Scanning 13 (1991) 350.
[9] G. Demortier, S. Mathot, Nucl. Instr. and Meth. B 77 (1993) 312.
[10] R.A. Jarjis, Nuclear Cross Section Data for Surface Analysis, Vol. III, 1979, p. 231.
[11] U. Strombusch, W. Bakowsky, H. Lacek, Nucl. Phys. A 149 (1970) 605.
[12] G. Terwagne, G.G. Ross, L. Leblanc, J. Appl. Phys. 79 (1996) 8886.
[13] L.R. Doolitlle, Nucl. Instr. and Meth. B 9 (1985) 344.